Effects of Temperature and pH on the Contraction and Aggregation of Microgels in Aqueous Suspensions

Nodar Al-Manasir,[†] Kaizheng Zhu,[†] Anna-Lena Kjøniksen,[†] Kenneth D. Knudsen,[‡] Göran Karlsson,[§] and Bo Nyström*,[†]

Department of Chemistry, University of Oslo, P.O. Box 1033, Blindern, N-0315 Oslo, Norway, Department of Physics, Institute for Energy Technology, P.O. Box 40, N-2027 Kjeller, Norway, and Department of Physical and Analytical Chemistry, Uppsala University, Box 579, S-751 23 Uppsala, Sweden

Received: February 6, 2009; Revised Manuscript Received: July 2, 2009

Chemically cross-linked poly(*N*-isopropylacrylamide) (PNIPAM) microgels and PNIPAM with different amounts of acrylic acid groups (PNIPAM-*co*-PAA) were synthesized and the temperature-induced aggregation behaviors of aqueous suspensions of these microgels were investigated mainly with the aid of dynamic light scattering (DLS) and turbidimetry. The DLS results show that the particles at all conditions shrink at temperatures up to approximately the lower critical solution temperature (LCST), but the relative contraction effect is larger for the microgels without acid groups or for microgels with added anionic surfactant (SDS). A significant depression of the cloud point is found in suspensions of PNIPAM with very low concentrations of SDS. The compression of the microgels cannot be traced from the turbidity results, but rather the values of the turbidity increase in this temperature interval. This phenomenon is discussed in the framework of a theoretical model. At temperatures above LCST, the size of the microgels without attached charged groups in a very dilute suspension is unaffected by temperature, while the charged particles (pH 7 and 11) continue to collapse with increasing temperature over the entire domain. In this temperature range, low-charged particles of higher concentration and particles containing acrylic acid groups at low pH (pH 2) aggregate, and macroscopic phase separation is approached at higher temperatures. This study demonstrates how the stabilization of microgels can be affected by factors such as polymer concentration, addition of ionic surfactant to particles without charged acid groups, amount of charged groups in the polymer, and pH.

Introduction

Synthetic monodisperse stimuli-responsive microgels in the nano- to micrometer-size range continue to attract attention due to their potential applications[1] in numerous fields, including drug delivery,[2−5] chemical separations,[6,7] sensors,[8,9] catalysis,[10,11] and enhanced oil recovery.[12] The large amount of applications of microgels arise from their stimuli-responsive nature, that is, their ability to undergo reversible volume phase transitions in response to environmental stimuli such as temperature,[13] pH,[14−16] and ionic strength.[17]

Polymer microgels are physically or chemically cross-linked particles with a network structure that is swollen in a suitable solvent. This category of substances is classified as "smart or intelligent materials" because these microgels can undergo conformation changes in response to alterations in environmental conditions. In the preparation of polymeric microgel particles, there are in principle four methods that have been reported, namely emulsion polymerization,[18] anionic copolymerization,[19] chemical cross-linking of neighboring chains,[20] and microemulsion polymerization.[17] The most studied class of responsive polymers are temperature sensitive poly(acrylamide), specifically poly(*N*-isopropylacrylamide) (PNIPAM). This polymer undergoes thermally induced deswelling when the solution temperature is raised above the lower critical solutions temperature (LCST for aqueous solutions of PNIPAM is approximately 32 °C[21]). At temperatures well below the LCST, PNIPAM is highly solvated owing to hydrogen bonding between water molecules and amide residues of the polymer chains. The hydrogen bonding with water is increasingly disrupted on heating causing water to act as a poorer solvent for PNIPAM, leading to gradual chain collapse. However, the hydrophobicity of the polymer is enhanced at elevated temperatures, and this effect can easily lead to multichain association and the growth of huge aggregates. As a result, heating of an aqueous suspension of chemically cross-linked PNIPAM microgels can evoke a situation where intrachain contraction is overshadowed by interpolymer aggregation at high temperatures.

Morphology, swelling, and kinetics of this type of microgels have attracted a great deal of interest, and several papers[13,22,23] have appeared in recent years. Another subject that has been studied thoroughly over the years is the stabilization and aggregation[24] of microgel particles. The effect of surfactant addition to PNIPAM has also been reported in several papers.[25] It has been established that swelling is promoted by SDS addition, and polymer−surfactant aggregates are formed. However, a systematic study of contraction and aggregation of PNIPAM containing microgels under various conditions by using different experimental techniques is still lacking. Important effects for swelling and stabilization of microgels that are addressed in this work are particle concentration, introduction of charged moieties in PNIPAM, pH influence, and addition of ionic surfactant to suspensions of PNIPAM. To obtain a concise picture of these

* To whom correspondence should be addressed.
[†] University of Oslo.
[‡] Institute for Energy Technology.
[§] Uppsala University.

10.1021/jp901121g CCC: $40.75
Published on Web 07/20/2009

TABLE 1: Characteristic Feed Ratio Data and Values of the Zeta-Potential for the Synthesized Temperature- and pH-Responsive Microgels

sample code	[NIPAAM] (mol %)	[BIS] (mol %)	[AA] (mol %)	electrophoretic mobility ($cm^2/(Vs) \times 10^{-4}$) ± SD
MG-01	92	2	6	-1.83 ± 0.06
MG-02[a]	92	2	6	-1.98 ± 0.09
MG-03	98	2	0	-0.81 ± 0.06
MG-04	97	2	1	-1.22 ± 0.03

[a] The only sample that was synthesized in the presence of SDS (60 mg).

effects, it is important to gain a better insight into the delicate interplay of intrachain and interparticle aggregation.

The aim of the present investigation is to elucidate in a systematic way the intricate competition between temperature- or pH-induced hydrophobic association and repulsive electrostatic forces on the contraction and aggregation of nanoparticles at various conditions. In the past, the attention has been focused on either swelling or stability of the particles, but much less interest has been paid to the combination of these effects and the impact of thermodynamics on the flocculation process. A more precise understanding of this interplay will allow us to come up with a strategy to control temperature-induced interparticle aggregation.

For this purpose, we have synthesized PNIPAM microgels cross-linked by *N*,*N*′-methylenebis(acrylamide) (BIS) and charged PNIPAM with different amounts of acrylic acid groups (PNIPAM-*co*-PAA). The characteristic data for the microgels are presented in Table 1. The results will demonstrate that the interplay between intrapolymer and interpolymer aggregation can be tuned by changing factors such as the concentration of PNIPAM, incorporate charged groups onto the PNIPAM chains, or adding an ionic surfactant to a solution of PNIPAM. In addition, effect of pH on the temperature-induced association behavior is analyzed. We believe that the findings from this work provide us with a better understanding of the intricate competition between intrachain and interchain association in systems of thermally sensitive polymers.

Experimental Section

Materials. *N*-Isopropylacrylamide (NIPAM, Acros) was recrystallized from a toluene/hexane mixture solvent and dried at room temperature under vacuum prior to use. *N*,*N*′-methylenebis(acrylamide) (BIS), ammonium persulfate (APS), acrylic acid (AA), and sodium dodecyl sulfate (SDS) were utilized in the preparation of microgel samples, and all chemicals were purchased from Sigma-Aldrich, Norway AS and used as received. The chemicals—H_3PO_4, NaH_2PO_4, Na_2HPO_4, and Na_3PO_4—were used to prepare the buffer systems employed in this work, and they were all purchased from Sigma-Aldrich. Buffered solutions at pH values of 2, 7, and 11 were utilized in this study. All the buffers were prepared with a total molarity of 0.05 M. The water employed in this investigation was purified with a Millipore Milli-Q system, and the resistivity was approximately 18 MΩ cm.

Microgel Synthesis. A detailed route for preparation of microgels by free radical precipitation polymerization has been reported elsewhere.[26] A typical procedure can be briefly described in the following way. The total concentration of the monomers in the pregel sample was kept constant at 70 mM, where 2 mol % was BIS, 6 mol % was acryl acid (AA), and the remaining 92 mol % was NIPAM. All monomers were dissolved in 600 mL of water, and the resulting solution was filtered through a 0.1 μm membrane filter to remove particulate matter. The reaction mixture was first purged with nitrogen for 30 min to remove the dissolved oxygen in a 1-L 3-neck round-bottom flask, equipped with a condenser and inlet for nitrogen. The mixture was then heated to 70 °C under a gentle stream of nitrogen for 1 h, after which 60 mg of APS dissolved in 5 mL of degassed water was added to initiate the reaction. The reaction mixture became turbid about 1 min after the APS solution was added. The reaction mixture was kept at 70 °C for another 4 h to complete the reaction. After cooling, the reaction mixture was kept at room temperature and the microgel solution was filtered using fine porosity filter paper (Schleicher & Schuell GmbH) to remove possible aggregated material. The particles were then further purified by dialysis (Spectra/Por 6 dialysis membrane, MWCO 8000) against water that was changed daily for at least 4 weeks to remove low-molecular weight impurities such as unreacted monomers, as well as minute rests of SDS (for MG-02*) from the microgels. The microgel products were finally collected by lyophilization. It should be mentioned that in the preparation of one sample (MG-02*), the polymerization reaction was conducted in the presence of SDS.

We note from Table 1 that the microgel particles have the same degree of cross-linking and the NIPAM contents are almost the same. As frequently reported, the free radical precipitation polymerization produces nearly monodispers spherical particles in the submicrometer size range.[26,27] One type of particles (MG-03) was synthesized from a mixture of only NIPAM and the cross-linker (BIS), and these microgels consist of only cross-linked NIPAM chains without incorporated acid group and one sample (MG-04) has a few acid groups. The two other microgel types (MG-01 and MG-02*) have both 6 mol % of charged acid groups, but the MG-02* sample was prepared in the presence of SDS. As shown below, the microspheres from MG-02* have a smaller size than all of the other types of microspheres because SDS can better stabilize the small precursor particles.[28] We note that the microgels have different electrophoretic mobility, with the highest value for the sample prepared in the presence of SDS and the lowest for the particles without acid groups. This suggests that the MG-02* spheres have the highest capacity to resist aggregation, whereas flocculation is more feasible for the MG-03 spheres at elevated temperatures. The polymerization reaction and the simple chemical structure of the PNIPAM-*co*-PAA system are depicted in Figure 1.

Turbidimetry. Influence of temperature on the transmittance of aqueous suspensions of the studied microgel systems was measured with a temperature controlled Helios Gamma (Thermo Spectronic, Cambridge, UK) spectrophotometer at a wavelength of 500 nm. The apparatus is equipped with a temperature unit (Peltier plate) that gives a good temperature control over an extended time. In this work, the heating rate in most of the experiments was set to 0.2 °C/min, and no effect of the heating rate on the signal was observed at low heating rates. The heating rate of the spectrophotometer was controlled by a PC that was interfaced to the apparatus and equipped with homemade software that gives the possibility of performing both temperature and wavelength scans with user-defined protocols.

The turbidity τ of the samples can be determined from the following relationship: $\tau = (-1/L) \ln(I_t/I_0)$ where L is the light path length in the cell (1 cm), I_t is the transmitted light intensity, and I_0 is the incident light intensity. The results from the spectrophotometer measurements will be presented in terms of turbidity.

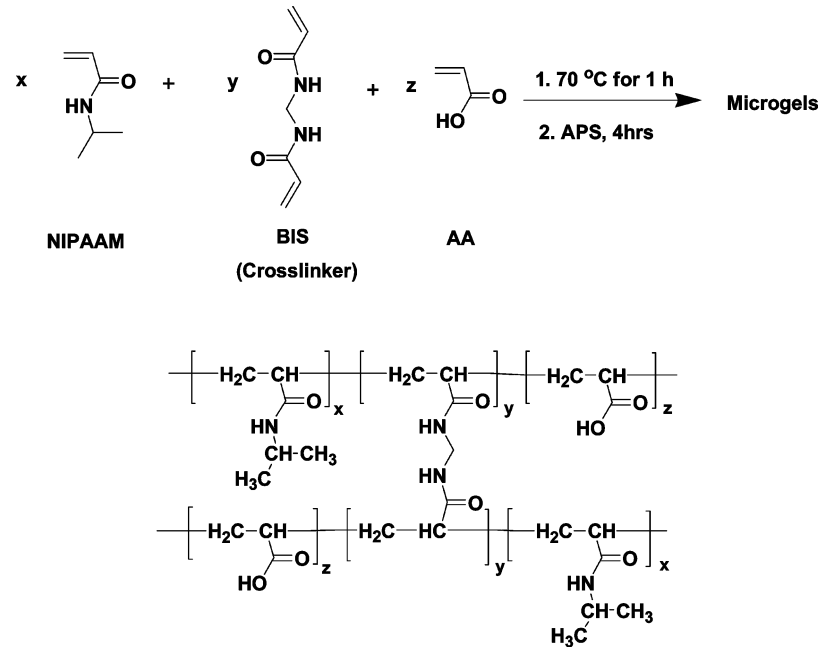

Figure 1. Schematic illustration of the synthesis and chemical structure of the cross-linked PNIPAM-*co*-PAA microgel system.

Dynamic Light Scattering. In light scattering experiments we probe on a length scale of q^{-1}, where q is the wave vector defined as $q = 4\pi n \sin(\theta/2)/\lambda$. Here λ is the wavelength of the incident light in a vacuum, θ is the scattering angle, and n is the refractive index of the medium.

The dynamic light scattering (DLS) experiments were conducted with the aid of an ALV/CGS-8F multidetector version compact goniometer system, with 8 fiber-optical detection units, from ALV-GmbH., Langen, Germany. The beam from a Uniphase cylindrical 22 mW HeNe-laser, operating at a wavelength of 632.8 nm with vertically polarized light, was focused on the sample cell (10-mm NMR tubes, Wilmad Glass Co., of highest quality) through a temperature-controlled cylindrical quartz container (with 2 plane-parallel windows), vat (the temperature constancy being controlled to within ±0.01 °C with a heating/cooling circulator), which is filled with a refractive index matching liquid (*cis*-decalin). The polymer solutions were filtered in an atmosphere of filtered air through a 5 μm filter (Millipore) directly into precleaned NMR tubes. The DLS experiments were performed with a temperature gradient (0.2 °C/min) as for the turbidity measurements. The correlation function data were recorded continuously every 3 min. When going back to 25 °C after the heating cycle, the values were the same as before the sample was heated. In addition, quenching measurements with DLS, where the temperature was changed very fast from a high to a low temperature revealed that the transition from one state to another is a fast process.

In these dilute suspensions of microgels, the scattered field can be assumed to exhibit Gaussian statistics and the experimentally recorded intensity autocorrelation function $g^2(q,t)$ is directly linked to the theoretically amenable first-order electric field autocorrelation $g^1(q,t)$ through the Siegert[29] relationship $g^2(q,t) = 1 + B|g^1(q,t)|^2$, where B (≤ 1) is an instrumental parameter.

For suspensions containing particles with different size distribution, the nonexponential behavior of the autocorrelation function can be portrayed by using a Kohlrausch−Williams−Watts[30,31] stretched exponential function. This procedure has been reported[32−35] to be powerful in the analysis of correlation functions obtained from various colloid systems. This approach is also successful to describe the correlation function data in this work, and the algorithm employed in the analysis of the present correlation function data can be cast in the following form

$$g^1(t) = \exp[-(t/\tau_{fe})^{\beta}] \quad (1)$$

where τ_{fe} is some effective relaxation time and β ($0 < \beta \leq 1$) is a measure of the width of the distribution of relaxation times. The high values of β ($\beta \geq 0.94$) observed for the present microgel systems at all conditions suggest that the size distribution of particles is narrow and the particles are nearly monodisperse. The observation that $\beta \geq 0.94$ is also true in the stage when large clusters are evolved. The mean relaxation time is given by

$$\tau_f = (\tau_{fe}/\beta)\Gamma(1/\beta) \quad (2)$$

where $\Gamma(1/\beta)$ is the gamma function.

The correlation functions were analyzed by using a nonlinear fitting algorithm (a modified Levenberg−Marquardt method) to attain best-fit values of the parameters τ_{fe} and β appearing on the right-hand side of eq 1. A fit was considered to be satisfactory if there are no systematic deviations in the plot of the residuals of the fitted curve and the values of the residuals are small. Since the relaxation mode always is diffusive ($D = 1/\tau_f q^2$) for these systems, the apparent hydrodynamic radii R_h of the microgels can be calculated by using the Stokes−Einstein relationship

$$R_h = \frac{k_B T}{6\pi\eta D} \quad (3)$$

where k_B is the Boltzmann constant, T is the absolute temperature, η is the viscosity of the solvent, and D is the mutual diffusion coefficient. These suspensions become rather turbid

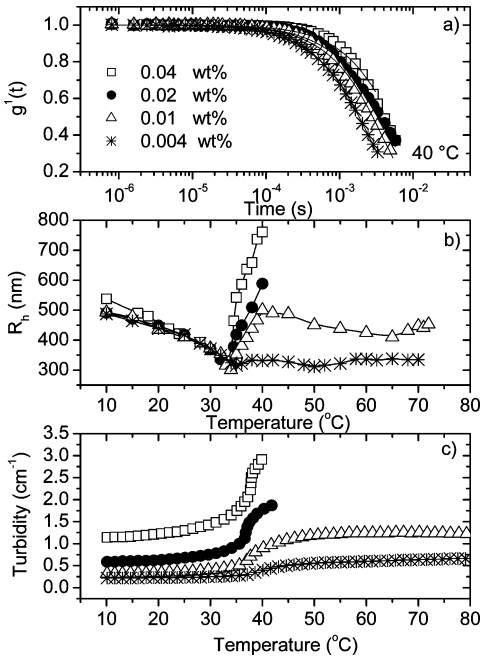

Figure 2. (a) First-order electric field correlation versus time (every second data point is shown) at a scattering angle of 90° for aqueous suspensions of PNIPAM microgels (MG-03) without acid groups of different concentrations at pH 7 and at a temperature of 40 °C. The solid lines are fitted to the data by means of eq 1. Temperature dependences of the apparent hydrodynamic radius (b) and the turbidity (c).

at elevated temperatures, and this may lead to problems with multiple scattering. However, at the conditions considered in this study, we have not detected any signs of this effect.

Results and Discussion

The stability of microgels is a vital issue in many applications, and below we will elucidate the delicate temperature-induced shrinking and aggregation of microgels at various conditions. Effects of polymer concentration, addition of an ionic surfactant, incorporation of different mol % of charged acrylic acid groups, and pH on the intra- and interpolymer association of microgel particles are discussed below.

Effect of Polymer Concentration. In Figure 2a, normalized time correlation function data at a scattering angle of 90° for aqueous suspensions of PNIPAM microgels of various concentrations at a temperature of 40 °C, together with the corresponding curves fitted with the aid of eq 1, are depicted in the form of semilogarithmic plots. Although enhanced aggregation occurs at this temperature for the higher polymer concentrations (cf. the discussion below), the decays can almost ($\beta \geq 0.94$) be described by a single exponential. This indicates a narrow distribution of sizes even when large clusters are formed. A comparison of the correlation functions clearly unveils a progressive slowing down of the relaxation process as the particle concentration increases. This tendency reflects the formation of large floc structures at this temperature and high concentration.

The general feature of R_h for all polymer concentrations is the marked collapse of the microgels at moderate temperatures (see Figure 2b). At low temperatures, the curves virtually condense onto each other, except for the highest polymer concentration where the augmented values of R_h indicate that some smaller aggregates have been formed even at low temperatures. The temperature-induced shrinking of the gel-particles can be accounted for in the following way. The isopropyl side group carried by each monomer of PNIPAM confers a degree of hydrophobic character, whereas the hydrophilic nature of the polymer is established through hydrogen bonding of water with the amide groups. At elevated temperatures, the hydrogen bonding with water is gradually disrupted on heating and the hydrophobicity of the polymer is enhanced with packing of the hydrophobic segments, leading to progressive chain collapse.[1,36] This contraction behavior of the microgels is redolent of the coil-to-globule transition reported[37−39] for single chains of high molecular weight of PNIPAM in very dilute solution.

At temperatures above the LCST (~32 °C), the temperature dependence of R_h is strongly affected by the polymer concentration, with an abrupt rise of R_h for the highest concentration and almost no effect of temperature on R_h for the lowest concentration. This finding can be rationalized in the following scenario. At elevated temperatures, a situation of a perpetual competition between contraction of the microgels and flocculation evolves. At temperatures above the LCST, the hydrophobic stickiness of the species is enhanced and the higher sticking probability at high concentration promotes the formation of large aggregates. For the higher two concentrations, aggregation is the predominant phenomenon at elevated temperatures and macroscopic phase separation is approached, in spite of that the particles carry some charges (see Table 1). However, for an intermediate polymer concentration of 0.01 wt % the delicate interplay between building up interpolymer complexes and intrachain shrinking is reflected by the peak centered on 40 °C (Figure 2b). For the lowest concentration, the collision frequency of spheres is low and the tendency of forming aggregates is repressed. These results clearly show that intrachain contraction and c coexist at elevated temperatures for particles with a low charge density, and these features are strongly governed by the particle concentration.

It has been argued that microgels exhibit core−shell morphology and that the overall deswelling at elevated temperatures is essentially governed by the contraction of the outer regions of the particle.[23] As a consequence, the hydrophilic corona becomes thin and this facilitates interparticle aggregation through hydrophobic interactions.

The effect of temperature on the turbidity (τ) for suspensions of PNIPAM of various concentrations is depicted in Figure 2c. The general picture that emerges is that the turbidity values at low temperatures increase with particle concentration, and the transition zones, with enhanced values of τ, for the different polymer concentrations are located at approximately the same temperatures as the corresponding alterations of R_h occur. Due to the absence of a developed plateau region in the turbidity curves at low temperatures (Figure 2c), it is difficult to determine an accurate cloud point (CP) but the general trend is that the value of CP decreases as the particle concentration rises. For the higher two concentrations the upturn of τ is strong at high temperatures, suggesting development of huge clusters and phase separation. At the lower concentrations, the turbidity curves level out at high temperatures. This trend indicates that the growth and collapse of the species cancel each other.

In the analysis of the turbidity results, we may resort to theoretical approaches[40,41] elaborated for spherical colloidal particles. The following expression was derived[41] for the turbidity $\tau = 3cQ_{ext}/(2d\rho)$, where c is the mass concentration (g/cm^3), Q_{ext} is the Mie extinction efficiency, d is the particle diameter, and ρ is the density of the particles. It is reasonable to assume at temperatures below the LCST that the mass m of

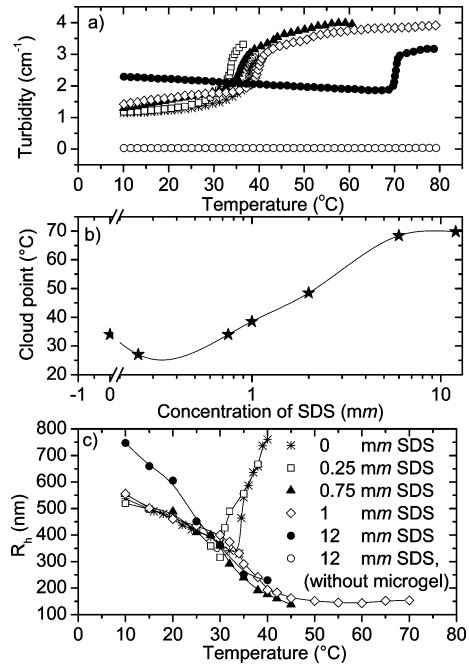

Figure 3. (a) Temperature dependence of the turbidity for an aqueous suspension (0.04 wt %) of PNIPAM microgels (in the absence of acid groups) at the levels of SDS addition indicated and at pH 7. (b) Effect of SDS concentration on the cloud point. (c) Temperature dependence the apparent hydrodynamic radius.

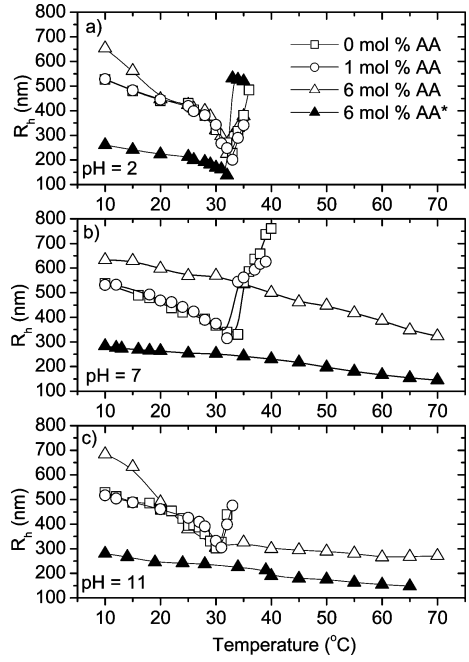

Figure 4. Plot of the apparent hydrodynamic radius as a function of temperature for 0.04 wt % suspensions of PNIPAM and PNIPAM-*co*-PAA, with different mol % of the acrylic acid (AA) groups, at the pH values indicated in buffer systems of a total molarity of 0.05 M. The asterisk (6 mol % AA*) in the inset denotes the sample that has been synthesized in the presence of SDS.

the spherical particles of volume V is constant. In view of this, we can write $\rho = m/V$, where $V = (4/3)\pi(d/2)^3$. By inserting this in the expression above, we arrive at $\tau = cQ_{ext}\pi d^2/4m$. This relation readily explains the raise of τ with increasing polymer concentration, and the strong increase of τ upon augmented aggregation at higher concentrations and temperatures. However, the significant temperature-induced collapse of the microgels observed from the DLS experiments at temperatures below the LCST (the average size of the microgels decreases from approximately 500 to 300 nm in the temperature interval from 10 to 33 °C) is not directly reflected in the turbidity data (Figure 2c). To interpret this result in the framework of the equation above, it is necessary to argue that the value of Q_{ext} should increase with increasing temperature because c and m for a given concentration should be constant. The parameter Q_{ext} cannot easily be determined experimentally, but its value is a function of the relative refractive index n_p/n_0 (n_p is the refractive index of the spherical particle and n_0 is the refractive index of the solvent), and the value of Q_{ext} increases with increasing value of the quantity n_p/n_0. It is not unreasonable to presume that the refractive index of the particles increase during the compression stage, and this can therefore lead to an increase of τ in the initial stage (from 10 to 33 °C). To elucidate the impact of a change of the relative refractive index, it may be instructive to consider a relevant example and use the data presented in Figure 2a in ref 41. If we use the same wavelength ($\lambda = 500$ nm) as in the present turbidity measurements, the ratio $\pi d/\lambda$ (on the x axis in Figure 2 of ref 41) is altered from 3.1 to 1.9 as the particle size is changed from 500 to 300 nm. If we assume that the corresponding value of n_p/n_0 is changed from 1.05 to 1.10, the value of τ is increased by almost a factor of 2, in spite of that the size of the microgel drops from 500 to 300 nm. For the highest polymer concentration (0.04 wt %) considered here, the increase observed for the value of τ is ca. 30% in the interval from 10 to 33 °C. This indicates that the variation of the value of n_p/n_0 upon the temperature-induced compression is less than in the invented example above.

Effect of Surfactant Addition. When an ionic surfactant such as SDS is added to a PNIPAM system, it has been argued[42] that the isopropyl side group carried by each monomer of PNIPAM is responsible for the interaction and binding of SDS to the polymer. The adsorption of the anionic SDS endows a polyelectrolyte character of PNIPAM, and it is also possible that some hydrophobic moieties are solubilized by the addition of SDS.

Figure 3a shows the effect of temperature on the turbidity for PNIPAM (MG-03) in the presence of different levels of SDS addition. A conspicuous feature is the temperature-induced rise of the turbidity at higher temperatures, and as the concentration of SDS increases the transition is shifted toward higher temperatures as a result of higher charge density on the surfaces of the particles when SDS is adsorbed and also solubilization of hydrophobic moieties of PNIPAM. Again, the temperature-induced compaction of the microgels is accompanied by an increase of τ at all levels of surfactant addition, except at the highest SDS concentration. This rise of τ can be explained in a framework similar to that described above, namely that compression of the species lead to a situation where the relative refractive index of the particles is increased and this leads to higher values of Q_{ext}. However, at the highest SDS concentration τ decreases slightly in the temperature interval from 10−70 °C, which probably can be attributed to the very strong compression of the microgels (from ca. 750 to 150 nm). The higher values of τ for PNIPAM in the presence of surfactant, especially at the highest surfactant concentration, can probably be ascribed to expansion due to solubilization of the hydrophobic moieties and electrostatic repulsive interactions. In the absence of microgels, the turbidity of aqueous solutions of SDS is very low and not affected by temperature in the considered interval.

A close inspection of the turbidity data and the cloud point (CP) results (Figure 3b) reveals a novel and amazing depression

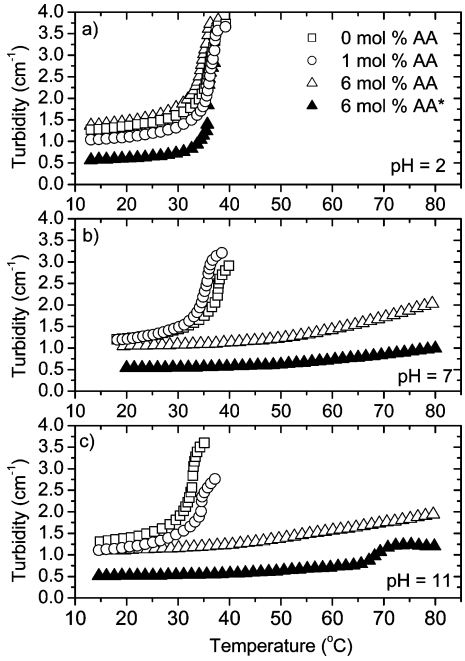

Figure 5. Temperature dependences of the turbidity for 0.04 wt % suspensions of PNIPAM and the PNIPAM-*co*-PAA copolymer, with different mol % of the acrylic acid (AA) groups, at the pH values indicated in buffer systems with a total molarity of 0.05 M. The asterisk (6 mol % AA*) in the inset text denotes the sample that has been synthesized in the presence of SDS.

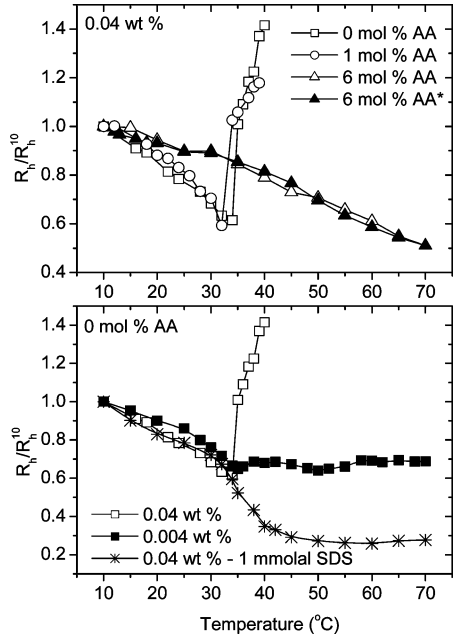

Figure 6. Temperature dependences of the relative hydrodynamic radius for the systems indicated at pH 7. See text for details.

of the CP at a low level (0.3 mm) of SDS addition. This finding suggests that a small addition of SDS promotes the sticking probability and aggregates are formed at a lower temperature when in the absence of surfactant. At levels of SDS addition above 0.3 mm SDS the value of CP increases monotonously with increasing SDS concentration up to about 8 mm SDS where CP levels off. This indicates that both enhanced charge density of the particles and solubilization of hydrophobic moieties postpone the aggregation process to higher temperatures. The fact that the cloud point curve flattens out at high levels of surfactant addition is consistent with a study[25] on binding isotherms of SDS to PNIPAM, where the SDS binding to the polymer slowly increased above the CMC (ca. 8 mM) with increasing surfactant concentrations.

The origin of the depression of CP at low SDS concentrations is not clear, but it is possible that the surfactant concentrations are below the critical aggregation concentration (CAC) at which the surfactant is adsorbed onto the microgel particles and thereby increases the charge density of the particles. It has been observed[25] previously that the SDS binding to PNIPAM is small at low levels of SDS addition, but the SDS binding increased sharply above an equilibrium SDS concentration of 3 mM. This lends support to our hypothesis that the lowest concentration of SDS is below CAC. Our conjecture is that a small amount of added SDS may lead to a weakening of the hydrogen bonds and in that way favor interparticle aggregation at a lower temperature. In this context it should be mentioned that a similar effect was reported[43] for ethyl(hydroxyethyl)cellulose (EHEC), which is an amphiphilic polysaccharide with a lower critical solution temperature at about 34 °C. In this case, the minimum of the cloud point curve that was located at approximately 2 mm SDS was ascribed to enhanced polymer−surfactant interactions as the CAC (≈ 2 mm) of the system was approached.

Effects of temperature on the apparent hydrodynamic radius for PNIPAM (MG-03) microgels at different levels of SDS addition are illustrated in Figure 3c. In the absence of SDS or at low levels of surfactant, the particles are initially compressed and at higher temperatures interparticle aggregates are evolved. An inspection discloses that the growth of the clusters occurs at a lower temperature for the sample with 0.25 mm SDS than for that without SDS. This is consistent with the lowering of CP, and it indicates that a very low SDS concentration promotes aggregation at a lower temperature. At intermediate surfactant concentrations, the PNIPAM microgels contract from approximately 550 to 150 nm, and at higher temperatures the value of R_h is virtually unaffected by temperature. This observation discloses that over the studied temperature domain, the microgels collapse and no growth of aggregates is detected at high temperatures because the particles are decorated by SDS molecules, which generate electrostatic repulsive forces and thereby electrostatically stabilize the particles against aggregation. It is possible that some of the hydrophobic stickers are solubilized, and this may lead to reduced stickiness of the particles. The first study on the influence of surfactants on the compression and stability of PNIPAM microgel was by Tam et al.[44]

At the highest SDS concentration (12 mm), a pronounced swelling of the particles is observed at low temperatures. It has been shown[25,44] that at higher levels of SDS addition, the particles swell much more than in surfactant-free suspension media due to electrostatic interactions.

Influence of Charge Density and pH on the Association Behavior. To scrutinize the influence of charge density and pH on the association behavior of the temperature sensitive polymer, DLS and turbidity measurements have been conducted on 0.04 wt % suspensions of PNIPAM and charged PNIPAM-*co*-PAA, with different mol % of the acrylic acid groups (AA), in buffer systems of a total molarity of 0.05 M at pH values covering both the acid and basic domain. In addition, experiments have been carried out on a PNIPAM-*co*-PAA sample, with 6 mol % acrylic acid groups, which have been synthesized in the presence of SDS. The results from DLS are collected in Figure 4. Let us first discuss the influence of charge density on the size of the microgels at neutral (pH 7) conditions (Figure 4b). A low charge

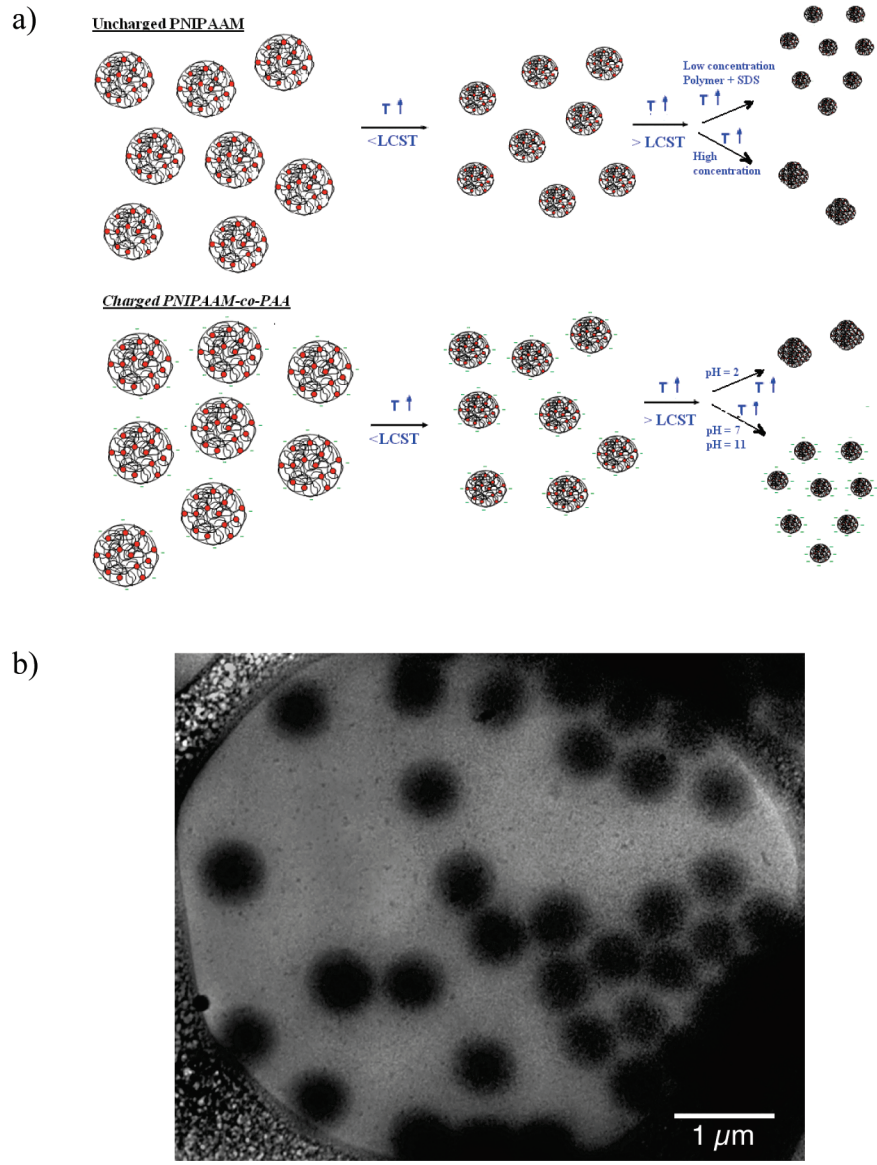

Figure 7. (a) Schematic illustration of effects of polymer concentration, SDS addition, pH, and charge density on the temperature-induced aggregation behavior of microgels. (b) Cryo-TEM image of a 0.04 wt % suspension of uncharged PNIPAAM microgels at 38 °C. The scale bar is 1 μm.

density (1 mol % AA) has practically no effect on the temperature dependence of R_h. For the PNIPAM with 6 mol % AA groups, the particles swell at low temperatures owing to deprotonation of the carboxylic acids and the resultant electrostatic repulsion between the negatively charged carboxylate residues (pK_a of AA is ca. 4.25),[45] whereas at higher temperatures a monotonous compression of the species takes place as the temperature increases as consequence of disruption of hydrogen bonds and enhanced hydrophobic interaction. The charges on the surfaces of the microgels suppress the tendency of forming aggregates. For the PNIPAAM-*co*-PAA sample (6 mol % AA) that has been synthesized in the presence of SDS, the values of R_h are significantly lower than for the other samples and the microgels are compressed as the temperature increases. It is well-known[1,16] that a surfactant as SDS acts as an efficient stabilizer of the particles during the cross-linker reaction and preventing the particles from coagulating.

At acid conditions (pH 2) and low temperatures, R_h exhibits a pronounced drop at moderate temperatures that is similar as that for the sample at neutral pH, but in this case all systems show macroscopic phase separation slightly above the LCST (~32 °C; see Figure 4a). It has been argued[46] that coagulation at low pH values is ascribed to a marked difference between the Haamaker constants of the microgels and liquid medium owing to condensation of the particles and reduced electrostatic stabilization (through neutralization of COO^-).

At strongly basic conditions (pH 11), the main features of R_h are similar as those at neutral pH (see Figure 4c). At higher pH values, the microgels are expected to swell because of the ionization of the carboxylic acid groups. A close inspection of the data, actually reveals that the values of R_h at low temperatures for the PNIPAAM with 6 mol % AA groups are higher than the corresponding ones at pH 7. At temperatures above LCST, the corresponding values of R_h are lower at pH 11, because of more effective stabilization of the particles at a higher degree of ionization.

Figure 5 shows temperature dependences of the turbidity at different pH values for 0.04 wt % suspensions of the unmodified PNIPAM and the PNIPAM-*co*-PAA copolymer, with different mol % of the AA groups. A general feature at all pH values is the sharp transition of the turbidity at temperatures slightly above LCST for the samples with low charge density (0 and 1 mol % AA). This announces the formation of giant clusters of particles. At pH 2, the most conspicuous feature is the abrupt temperature-

induced transition for all systems, illustrating the strong aggregation of the particles in the suspensions. At low temperatures, the results are compatible with the DLS finding that smaller microgels are developed when the particles are prepared in the presence of SDS. At pH 7 and 11, the values of τ for the systems with 6 mol % AA groups, both with and without added SDS in the preparation of the microgels, show moderate upturns at high temperatures. This suggests that the tendency of forming large aggregates is reduced due to charge stabilization of the microgels.

To illustrate the relative change of the apparent hydrodynamic radius with temperature for the different microgels at pH 7, the quantity R_h/R_h^{10} (R_h^{10} is the hydrodynamic radius at a temperature of 10 °C) is plotted as a function of temperature in Figure 6. This illustration divulges that up to the LCST, the compression of the particles is more prominent for the systems of low charge density because when the number of charges is high, the charges inside the microgels will give rise to repulsive forces that counteract the intrachain contraction. At higher temperatures, the microgels of systems with higher charge densities are decorated with charges onto the surfaces, and this provides the stability of the suspension. It is obvious from Figure 6 (the lower panel) that the temperature-induced compression of the microgels is much stronger in the presence of SDS, even when the suspension without added SDS is very dilute. This reflects that though the collision frequency is low some aggregates are formed.

Effects of polymer concentration, pH, and charge density on the temperature-induced association behavior of microgels are schematically illustrated in Figure 7. The illustration shows that contraction always happens at temperatures below the LCST. We note that at temperatures above the LCST, the slightly charged microgels form aggregates, except at very low concentrations or in the presence of SDS. Intuitively, we would expect that when big aggregates are formed at elevated temperatures for a sample containing many microgel particles, species of various sizes should exist in the suspension. However, values of the stretched exponential β close to 1 at this stage, suggests that the size distribution is narrow.

To obtain more information about the species, we have carried out a few cryogenic transmission electron microscopy (cryo-TEM) measurements on 0.04 wt % of uncharged PNIPAM microgels at a temperature of 38 °C (large aggregates ($R_h \approx$ 650 nm) are formed). The experimental technique and the instrumentation have been described elsewhere,[47] as well as the performance of the measurements.[48] The results demonstrate (see Figure 7b) that huge spherical particles are formed with a narrow size distribution. This finding supports the DLS results that the species are nearly monodisperse, even in a stage not far from phase separation. Particles with diffuse outer rim indicate that uniform loosely aggregated species are formed. This finding indicates that the shells are quite tightly bound to the core particles.[24]

Conclusions

Chemically cross-linked PNIPAM microgels, together with analogous (PNIPAM-*co*-PAA) copolymers were prepared and effects of particle concentration, temperature, surfactant addition, and pH were scrutinized with the aid of dynamic light scattering and turbidimetry. At temperatures up to the LCST all the studied microgels were observed to shrink, independent of polymer concentration, surfactant addition, incorporated acid groups, and pH. The turbidity and DLS results show that the tendency of forming aggregates at temperatures above LCST in suspensions of microgels with low charge density is repressed at low particle concentration. When aggregation takes place in suspensions of PNIPAM at elevated temperatures, results from cryo-TEM show that huge spherical particles are formed with a narrow size distribution. The latter finding is supported by the high values of β found from the analyses of the correlation functions from DLS.

An interesting and novel feature was observed in suspensions of PNIPAM with a very low concentration of SDS. In this case a pronounced depression of the cloud point was detected and interparticle aggregation started at a lower temperature than for the suspension without added SDS. At low temperatures, the size of the microgels in the presence of a high level of added SDS or with 6 mol % AA groups is appreciably larger than that of particles with a low charge density because of repulsive interactions. However, the microgels with 6 mol % AA groups that have been synthesized in the presence of SDS are much smaller than all the other microgels. The flocculation occurrence of PNIPAM at temperatures above LCST is strongly inhibited in the presence of SDS or when PNIPAM is equipped with acid groups.

At pH 2, all systems approach macroscopic phase separation at temperatures above the LCST. At pH 7 and 11, most of the features are similar and the results for the charged microgels (6 mol % AA and one with 6 mol % AA prepared in the presence of SDS) demonstrate that the apparent hydrodynamic radius drops continuously over the whole considered temperature range. This finding shows that the microgels are electrostatically stabilized. When the DLS measurements indicate that large aggregates evolve, this is accompanied by a marked upturn of the turbidity curve.

For suspensions of the charged PNIPAM-*co*-PAA microgels, the contraction of the particles continues over the entire temperature region at pH 7 and 11, whereas at pH 2 large clusters are formed above the LCST and macroscopic phase separation is approached.

Acknowledgment. We gratefully acknowledge support from the Norwegian Research Council for the projects 177665/V30 and financial support provided by VISTA/Statoil through the project "Screening of different generic types of polymers for possible use in enhanced oil recovery processes" (No. 6338).

References and Notes

(1) Saunders, R. S.; Vincent, B. *Adv. Colloid Interface Sci.* **1999**, *80*, 1.
(2) Jeong, B.; Bae, Y. H.; Lee, D. S.; Kim, S. W. *Nature* **1997**, *388*, 860.
(3) Castro Lopez, V.; Hadgraft, J.; Snowden, M. J. *Int. J. Pharm.* **2005**, *292*, 137.
(4) Das, M.; Zhang, H.; Kumacheva, E. *Annu. Rev. Mater. Res.* **2006**, *36*, 117.
(5) Oh, J. K.; Drumright, R.; Siegwart, D. J.; Matyjaszewski, K. *Prog. Polym. Sci.* **2008**, *33*, 448.
(6) Kawaguchi, H.; Fujimoto, K. *Bioseparation* **1998**, *7*, 253.
(7) Umeno, D.; Kawasaki, M.; Maeda, M. *Bioconjugate Chem.* **1998**, *9*, 719.
(8) Miyata, T.; Asami, N.; Uragami, T. *Macromolecules* **1999**, *32*, 2082.
(9) Holtz, J. H.; Asher, S. A. *Nature* **1997**, *389*, 829.
(10) Bergbreiter, D. E.; Case, B. L.; Liu, Y. - S.; Caraway, J. W. *Macromolecules* **1998**, *31*, 6053.
(11) Nagayama, H.; Maeda, Y.; Shimasaki, C.; Kitano, H. *Macromol. Chem. Phys.* **1995**, *196*, 611.
(12) Ju, B.; Fan, T.; Ma, M. *Chin. Particuol.* **2006**, *4*, 41.
(13) Pelton, R. H.; Pelton, H. M.; Morphesis, A.; Rowell, R. L. *Langmuir* **1989**, *5*, 816 See also. Hoare, T.; Pelton, R. *Macromolecules* **2004**, *37*, 2544.
(14) Garcia, A.; Marquez, M.; Cai, T.; Rosario, R.; Hu, Z.; Gust, D.; Hayes, M.; Vail, S. A.; Park, C.-D. *Langmuir* **2007**, *23*, 224.

(15) Bhattacharya, S.; Eckert, F.; Boyko, V.; Pich, A. *Small* **2007**, *3*, 650.
(16) Tan, B. H.; Tam, K. C. *Adv. Colloid Interface Sci.* **2008**, *136*, 25.
(17) Neyrer, S.; Vincent, B. *Polymer* **1997**, *38*, 6129.
(18) Clarke, J.; Vincent, B. *J. Chem. Soc. Faraday Trans.I* **1981**, *77*, 1831.
(19) Antionietti, M.; Pakula, T.; Bremser, W. *Macromolecules* **1995**, *28*, 4227.
(20) Frank, M.; Burchard, W. *Makromol. Chem. Rapid Commun.* **1991**, *12*, 645.
(21) Schild, H. K. *Prog. Polym. Sci.* **1992**, *17*, 163.
(22) Wu, X.; Pelton, R. H.; Hamielec, A. E.; Woods, D. R.; McPhee, W. *Colloid Polym. Sci.* **1994**, *272*, 467.
(23) Stieger, M.; Richtering, W.; Pedersen, J. S.; Lindner, P. *J. Chem. Phys.* **2004**, *120*, 6197.
(24) Rasmusson, M.; Routh, A.; Vincent, B. *Langmuir* **2004**, *20*, 3536.
(25) Mears, S. J.; Deng, Y.; Cosgrove, T.; Pelton, R. *Langmuir* **1997**, *13*, 1901.
(26) Jones, C. D.; Lyon, L. A. *Macromolecules* **2000**, *33*, 8301.
(27) Pelton, R. *Adv. Colloid Interface Sci.* **2000**, *85*, 1.
(28) Anderson, M.; Maunu, S. L. *J. Polym. Sci., Part B: Polym. Phys.* **2006**, *44*, 3305.
(29) Siegert, A. J. F. Massachusetts Institute of Technology, Rad. Lab. Rep. No. 465, 1943.
(30) Kohlrausch, R. *Prg. Ann. Phys.* **1847**, *12*, 393.
(31) Williams, G.; Watts, D. C. *Trans. Faraday Soc.* **1970**, *66*, 80.
(32) Ngai, K. L. *Adv. Colloid Interface Sci.* **1996**, *64*, 1.
(33) Phillies, G. D. J.; Richardson, C.; Quinlan, C. A.; Ren, S Z. *Macromolecules* **1993**, *26*, 6849.
(34) Phillies, G. D. J.; Lacroix, M. *J. Phys. Chem. B* **1997**, *101*, 39.
(35) Kjøniksen, A.-L.; Joabsson, F.; Thuresson, K.; Nyström, B. *J. Phys. Chem. B* **1999**, *103*, 9818.
(36) Winnik, F. M. *Macromolecules* **1990**, *23*, 233.
(37) Wu, C.; Zhou, S. *Macromolecules* **1995**, *28*, 8381.
(38) Wu, C.; Wang, X. *Phys. Rev. Lett.* **1998**, *80*, 4092.
(39) Wang, X.; Qui, X.; Wu, C. *Macromolecules* **1998**, *31*, 2972.
(40) Heller, W.; Pangonis, W. J. *J. Chem. Phys.* **1957**, *26*, 498.
(41) Lechner, M. D. *J. Serb. Chem. Soc.* **2005**, *70*, 361.
(42) Jean, B.; Lee, L.-T.; Cabane, B. *Colloid Polym. Sci.* **2000**, *278*, 764.
(43) Kjøniksen, A.-L.; Knudsen, K. D.; Nyström, B. *Eur. Polym. J.* **2005**, *41*, 1954.
(44) Tam, K. C.; Ragaram, S.; Pelton, R. H. *Langmuir* **1994**, *10*, 418.
(45) Snowden, M. J.; Chowdhry, B. Z.; Vincent, B.; Morris, G. E. *J. Chem. Soc., Faraday Trans.* **1996**, *92*, 5013.
(46) Saunders, B. R.; Crowther, H. M.; Vincent, B. *Macromolecules* **1997**, *30*, 482.
(47) Almgren, M.; Edwards, K.; Karlsson, G. *Colloid Surf. A* **2000**, *174*, 3.
(48) Kjøniksen, A.-L.; Zhu, K.; Karlsson, G.; Nyström, B. *Colloid Surf. A* **2008**, *333*, 32.

JP901121G